Journal of Materials Chemistry C

Accepted Manuscript

ROYAL SOCIETY OF CHEMISTRY

rsc.li/materials-c

View Article Online
DOI: 10.1039/C8TC02823K

Journal Name

ARTICLE

Pyran-annulated perylene diimides derivatives as non-fullerene acceptors for high performance organic solar cells

Received 00th January 20xx,
Accepted 00th January 20xx

DOI: 10.1039/x0xx00000x

www.rsc.org/

Gang Li[‡a], Yu Zhang[‡a], Tao Liu[‡b]*, Shuaihua Wang[a],Dandan Li[a], Jiewei Li[*c], Fengting Li[d], Lian-Ming Yang[d], Zhenghui Luo[e], Chuluo Yang[e], He Yan[*b], Pin Hao[a], Qiaoyan Shang[a] and Bo Tang[*a]

There has been growing interest in the effectual strategy of constructing non-fullerene acceptors for organic solar cells that may overcome the defect of the traditional fullerene-based acceptors. Herein, two novel push-pull (acceptor-donor-acceptor) type small-molecule acceptors, that is, **TPA-PDI$_2$** and **TPA-PDI$_3$**, with triphenylamine (**TPA**) as the core unit and pyran-annulated perylene diimides (**Py-PDIs**) as peripheryl groups are designed and synthesized for non--fullerene organic solar cells (OSCs). After device optimization, OSCs based on **TPA-PDI$_3$** demonstrate good device performance with a power conversion efficiency (PCE) as high as 5.84%, surpassing the **TPA-PDI$_2$**-based counterparts fabricated under identical conditions (1.314% PCE). The high efficiency for **TPA-PDI$_3$** can be attributed to complementary absorption spectra with the donor material (**PBDB-T**), balanced carrier transport and favorable morphologies. To the best of our knowledge, this PCE of 5.84% is among the highest values based on ethynyl-functionalized **TPA**-shaped non-fullerene acceptors so far.

1. Introduction

Solution-processed organic solar cells(OSCs) have been widely investigated with great effort to convert solar energy into electrical energy with advantages of semi-transparency, lightweight, flexibility and large-area fabrication through low-cost solution-coatingmethods.[1] In generally, OSCs adopt a bulk heterojunction (BHJ) active layer consisting of a blend of donors and acceptors (fullerene derivatives).[2]However, the intrinsic drawbacks of the fullerene acceptors, such as weak absorption in visible region, high retail costs, inferior ambient stability and poor morphology stability, make it a problematic material for future practical application in OSCs. Therefore, nonfullerene acceptors(NFAs) used in OSCs have drawn vigorous attention from both academic and industry due to the advantages of tunable energy levels, strong absorption in the visible and even near-infrared region (vis-NIR), as well as easy purification compared to their fullerene counterparts.[3]

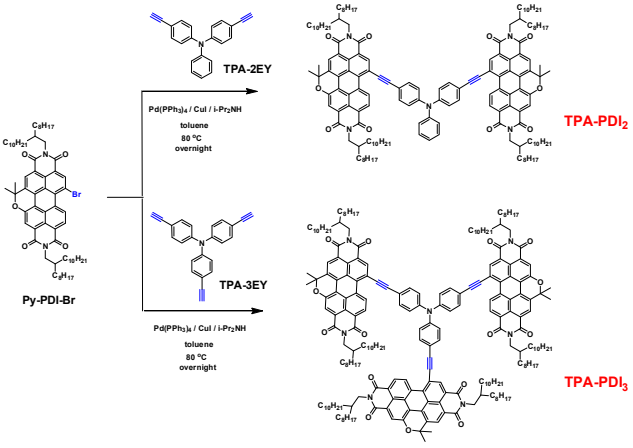

Scheme 1. Synthetic routes of **TPA-PDI$_2$** and **TPA-PDI$_3$**.

Up to date, series of high performance NFAs have been exploited,[4-5] especially for the systems of3,9-bis(2-methylene-(3-(1,1-dicyanomethylene)-indanone))-5,5,11,11-tetrakis(4hexylphenyl)-dithieno[2,3-*d*:2′,3′-*d*′]-*s*-indaceno[1,2-*b*:5,6-*b*′]-dithiophene (**ITIC**) and perylene diimides (**PDIs**). The PCE of organic solar cells based on the **ITIC** acceptors have exceeded 12%,[5h,6] while the record PCE of **PDIs**-based OSCs is 10.58%.[4f,5g] **PDIs** demonstrated several excellent properties,

[a.] College of Chemistry, Chemical Engineering and Materials Science, Key Laboratory of Molecular and Nano Probes, Ministry of Education, Collaborative Innovation Center of Functionalized Probes for Chemical Imaging in Universities of Shandong, Institute of Materials and Clean Energy, Shandong Provincial Key Laboratory of Clean Production of Fine Chemicals, Shandong Normal University, Jinan 250014, P. R. China. *E-mail: ligang@sdnu.edu.cn;tangb@sdnu.edu.cn
[b.] Department of Chemistry and Energy Institute, The Hong Kong University of Science and Technology, Clear Water Bay, Hong Kong. *E-mail: hyan@ust.hk; liutaozhx@ust.hk
[c.] Key Laboratory of Flexible Electronics (KLOFE) & Institute of Advanced Materials (IAM), Jiangsu National Synergetic Innovation Center for Advanced Materials (SICAM); Nanjing Tech University (NanjingTech), 30 South Puzhu Road, Nanjing, 211816, P.R. China. *E-mail: iamjwli@njtech.edu.cn
[d.] Beijing National Laboratory for Molecular Sciences (BNLMS), Key Laboratory of Green printing, Institute of Chemistry, Chinese Academy of Sciences, Beijing 100190, China.
[e.] Hubei Key Lab on Organic and Polymeric Optoelectronic Materials, Department of Chemistry, Wuhan University, Wuhan, 430072, China.
Electronic Supplementary Information (ESI) available: [Details of synthesis and characterization]. See DOI: 10.1039/x0xx00000x
‡ These authors contributed equally to the work.

View Article Online
DOI: 10.1039/C8TC02823K

such as easy functionalization, strong electron-acceptor character, finely tunable solubility, intense light absorption capability, energy level tunability, and self-assemblingproperties.[7] However, despite these favorable advantages, the strong tendency for π–π stacking between **PDIs** molecules inclined to form excessively large crystalline domains, which may result in large phase separation in active layers, thereby limiting the OSCs performance.[8]

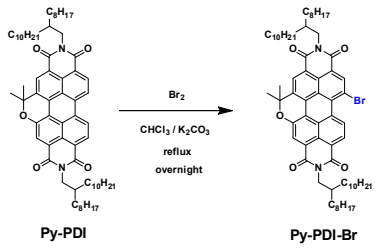

Scheme 2. Synthetic route of **Py-PDI-Br**.

Therefore, many strategies have been adopted to suppress the aggregation tendency to enhance the processability of the materials and to form favorable BHJ domain structures. Several groups devoted to the construction of twisted **PDIs** dimers and three-dimensional structure oligomers, connected by cores such as spirobifluorene,[9] tetraphenyletheylene,[8b] benzodithiophene[8a] and porphyrin.[10] Furthermore, S, Se and N heteroatoms had been incorporated at the bay positions of **PDIs** units to obtain more twisted structures and higher lowest unoccupied molecular orbital (LUMO) levels, which is favorable for achieving good device performances.[11] Therefore, further development of novel **PDIs** is worthy of being studied.

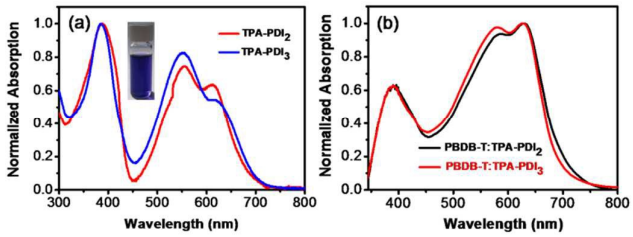

Figure 1. (a)The normalized absorption spectra of**TPA-PDI$_2$** and **TPA-PDI$_3$** in 10 μM dichloromethane solution. (b) The normalized absorption spectra of **PBDB-T: TPA-PDI$_2$** and **PBDB-T: TPA-PDI$_3$** blend films.

Recently, our group developed a novel pyran-annulated **PDIs** (**Py-PDIs**) which exhibited an extended UV-vis absorption and relatively high LUMO energy levels.[12] These properties demonstrated that **Py-PDIs** is a promising electron-deficient unit toward high-performance n-type semiconductors for OSCs. But the usage of **Py-PDIs** in non-fullerene organic solar cells has never been reported.

Herein we reported two novel propeller-shaped small molecule acceptor named **TPA-PDI$_2$** and **TPA-PDI$_3$** based on 3D-structured triphenylamine as the core which were flanked with acetylene unit and end-capped with **Py-PDIs**. By using **TPA-PDI$_3$** as the acceptors and the high performance polymer of **PBDB-T** (Fig.S17) as the donor, the highest PCE of 5.84% with an impressively high V_{oc} of 0.91 V, a J_{SC} of 10.27 mA/cm^2, a *FF* of 62.4%was achieved, which is 4.5 times higher than that of **TPA-PDI$_2$** (1.314% PCE). The results demonstrated that **Py-PDIs** is a good potential for the construction of high-performance non-fullerene acceptors.

2. Results and discussion

2.1. Synthesis and characterization

The synthetic routes of the two compounds are shown in Scheme 1 and 2.**Py-PDI-Br** was synthesized by bromination of compound **Py-PDI** under chloroform and potassium carbonateat reflux conditions (Scheme 2).The acetylene substituted **TPA** cores were synthesized according to the literature methods.[13] Target product of **TPA-PDI$_2$** and **TPA-PDI$_3$** were obtained in moderate yields by the palladium-catalyzed Sonogashira coupling reaction. The as-synthesized molecules were fully characterized by ^{1}H and ^{13}C NMR, Fourier Transform infrared spectroscopy (FT-IR), matrix assisted laser desorption ionization time of flight mass spectrometry (MALDI-TOF). Fig. S8 shows very sharp, well resolved peaks for the dimer, but the trimer (Fig. S10) shows very broad signals. We think the 3D molecular geometry enhanced the structural rigidity and conformational uniformity of the T**PA-PDI$_3$** molecule, which suppressed the free rotation of the **TPA** and **PDIs** leaded to a 3D interlocking structure. A similar interlocking conformation has been reported recently in a 3D **PDI**-based small molecule acceptor.[9] To verify the structure of the target product (**TPA-PDI$_3$**), we performed the MALDI-TOF measurements. (Fig. S13) and elemental analysis. Moreover, They show good solubility in common organic solvents, such as dichloromethane ,chloroform, and *o*-dichlorobenzene (*O*-DCB) at room temperature. These conjugated molecules also exhibit excellent thermal stability with a decomposition temperature (T_d, 5% weight loss) of 402 °C for **TPA-PDI$_2$** and 428 °C for **TPA-PDI$_3$** in nitrogen atmosphere. Obviously, the thermal stability of the two small molecules is adequate for their applications in OSCs.

2.2. Optical and electrochemical properties

The UV–vis absorption spectra of the two compounds in dichloromethane (DCM) solution(10^{-5}M) and as the solid film are presented in Fig. 1 and Fig. S1, and the corresponding data are summarized in Table S1. The two compounds exhibited similar absorption profiles. Compound**TPA-PDI$_3$** showed a strong visible absorption band in the wavelength range of 450-670 nm with a maximum molar extinction coefficient of 9.08 × 10^4M^{-1} cm^{-1} at 553 nm, which is higher than that of **TPA-PDI$_2$** (6.21 × 10^4M^{-1} cm^{-1} at 557 nm) most likely due to the synergistic effect of π–π interactions.[14]Neat **TPA-PDI$_2$** and **TPA-PDI$_3$** films display similar absorption spectra to their solution ones, indicating weak intermolecular aggregation in the solid state. The optical bandgap (E_g^{opt}) of two compounds were estimated to be 1.69 and 1.77 eV from the absorption onset of

View Article Online
DOI: 10.1039/C8TC02823K

their films. In addition, the absorption spectra of **TPA-PDI$_2$** and **TPA-PDI$_3$** with **PBDB-T** are well complemented to ensure a full harvest of light in the visible spectrum (Fig. 1b).

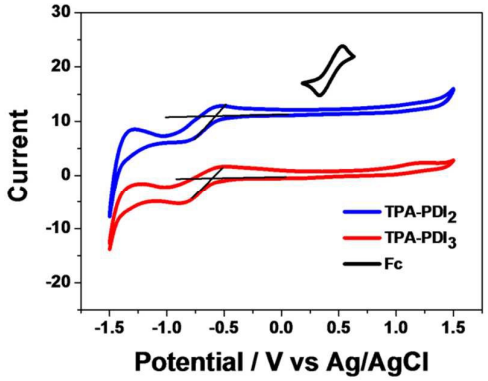

Figure 2. Cyclic voltammetry of **TPA-PDI$_2$** and **TPA-PDI$_3$** recorded in CH_3CN.

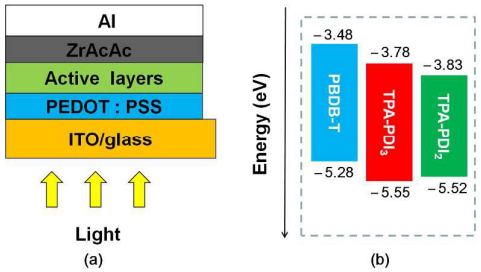

Figure 3. (a) Device configuration of the studied OSCs.(b) Estimated energy levels of **PBDB-T**, **TPA-PDI$_2$**, and **TPA-PDI$_3$** from electrochemical CV.Cyclic voltammetry of **TPA-PDI$_2$** and **TPA-PDI$_3$**thin films recorded in dry acetonitrile.

Cyclic voltammetry (CV) measurements were carried out to investigate the highest occupied molecular orbital (HOMO) and lowest unoccupied molecular orbital(LUMO) energy levels in CH_3CN solutions using Ag/Ag+ as a reference and Fc/Fc^+ (0.432 V) as a standard(Fig.2 and Table S1). The LUMO energy levels were calculated to be the onset of reduction potential,−3.83 and −3.78 eV, respectively, according to the equation $E_{LUMO} = -[q(E_{red} - E_{Fc/Fc+}) + 4.8)]$ eV.[15] The highest occupied molecular orbital (HOMO) energy levels for **TPA-PDI$_2$** and **TPA-PDI$_3$** were calculated to be −5.52 and −5.55 eV, respectively, according to the equation $E_{HOMO} = -(E_{LUMO} + E_g^{opt})$ eV.[15] As shown in Fig. 3b, the relatively high energy offsets of 1.5 eV (LUMO−LUMO) for **TPA-PDI$_3$** and **PBDB-T** compared with the counterpart of **TPA-PDI$_2$**and**PBDB-T** (1.45 eV) can produce a high V_{oc} for **TPA-PDI$_3$**-based PSCs.

2.3. Theoretical analysis

In order to gain a deeper insight on the geometric and electronic properties of the two acceptor molecules, density functional theory calculations were performed using the Gaussian package B3LYP/6-31G(d).[16]In order to facilitate the calculation, the long alkyl chains were replaced with an isopropyl group. The LUMO and HOMO orbitals are shown in Fig. S2. In**TPA-PDI$_2$**, the LUMO orbital localize in the PDIs unit While the HOMO electron density localizes in the **TPA** core along with **PDIs** unit. However, in**TPA-PDI$_3$**, the HOMO orbital concentrated in the core of **TPA**, implying obvious charge polarization in the excited state. The optimized molecular

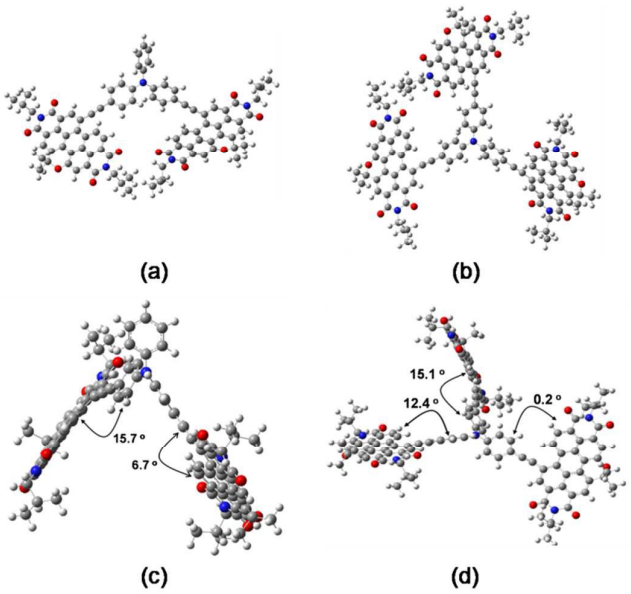

Figure 4. Optimized molecular geometries of **TPA-PDI$_2$** (a, c) and **TPA-PDI$_3$** (b, d) at B3LYP/6-31G(d).

geometries of two compounds are presented in Fig.4. The dihedral angles between **PDI** with benzene for **TPA-PDI$_2$** are 15.7° and 6.7°, respectively (Fig.4a, 4c). Another, the dihedral angles between **PDI** with benzene for **TPA-PDI$_3$** are 15.1°, 12.4° and 0.2°, respectively (Fig.4b, 4d). These results suggest that the introduction of the third **PDI** unit results in an obviously more twisted molecular configuration, which are expected to suppress aggregation to form favorable morphologies and nanoscale phase separation. The LUMO/HOMO energy levels of**TPA-PDI$_2$** and **TPA-PDI$_3$** are−3.33 /−5.27 eV and −3.39 /−5.34 eV through DFT calculations (Table S2), respectively. The calculated values are consistent with the values byCV measurements.

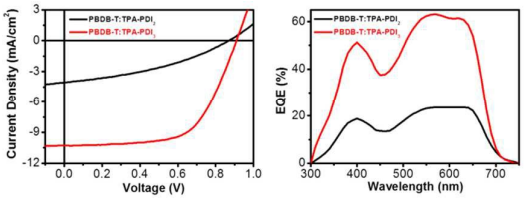

Figure 5. (a) *J - V* curves of BHJ OSCs based on **PBDB-T:TPA-PDI$_2$** (1:1, w/w),**PBDB-T:TPA-PDI$_3$** (1:1, w/w)without additive. (b) EQE curves of the corresponding BHJ OSCs.

2.4. Photovoltaic properties

View Article Online
DOI: 10.1039/C8TC02823K

Photovoltaic properties of**TPA-PDI$_2$** and **TPA-PDI$_3$** as acceptors were investigated in devices with a configuration of ITO glass/ poly(3,4-ethylenedioxythiopene):poly(styrene sulphonate) (PEDOT:PSS)/ active layers /ZrAcAc/Al were prepared. **PBDB-T** was chosen as the electron donor material because of complementary absorption to that of the two acceptors (See Fig. S17). The optimal conditions for preparing the devices were obtained by choosing the spin-coating speed and annealing temperatures carefully. The active layers were spin-coated from a solution in *o*-dichlorobenzene. The optimized weight ratio of D/A was 1:1, and the optimized thickness of the active layer is about 95 nm. The active layer is deposited at a spin-coating rate of 1600 rpm from their concentrated solutions (concentration, 20 mg mL^{-1}). The current density-voltage(J–V) curves of the OSCs with optimized devices under AM 1.5G, 100 mW/cm^2 are given in Fig. 5 and the corresponding photovoltaic parameters, V_{oc}, J_{sc}, FF and PCE of the devices are summarized in Table S3. Notably, the most efficient photovoltaic cells were obtained from the BHJ systems using**TPA-PDI$_3$** with **PBDB-T**, which showed a summit PCE of up to 5.84%with a $J_{sc}$of 10.27 mA cm^{-2}, and a V_{oc} of 0.91 V, an *FF* of 0.624. In contrast, the **TPA-PDI$_2$**- based OPVs exhibited PCE$_{max}$ = 1.314% with J_{sc}= 3.837 ±0.201 mA cm^{-2}, V_{oc}= 0.865±0.005 V, and *FF*= 0.368±0.004.We infer that the obvious enhancement in PCE values probably benefits from the improved charge transfer and superior morphology of the active layer, which decrease energy loss from charge recombination.

Fig. 5b shows the external quantum efficiencies (EQE) spectrum of the **TPA-PDI$_2$**and **TPA-PDI$_3$** based optimized OSCs. The J_{sc} values obtained by integrating the EQE curves with an AM1.5 G reference spectrum are in accord with those obtained from J–V measurements (within 5% mismatch). The optimized device showed a broad photo-to-current response from 350 to 680 nm with a maximum value of 67%and over 50% across the range of 500–650 nm, indicating a relatively efficient photoelectron conversion process.

2.5. Charge carrier mobility

To understand the difference of J_{sc} and *FF* of the different acceptor devices, the current–voltage (*J–V*) characteristics of blend films in space-charge-limited current (SCLC) devices were measured. The device structures of the electron only and hole only devices are ITO/ZnO/active layers /ZrAcAc/Al and ITO/V_2O_5/ active layers /V_2O_5/Al, respectively. The corresponding SCLC devices are shown in Fig. S3, and the corresponding electron/hole mobility data are listed in Table S4. The hole/electron mobilities for **PBDB-T: TPA-PDI$_2$** and **PBDB-T: TPA-PDI$_3$** blends are 5.65× 10^{-4} /2.23 ×10^{-4} cm^2 V^{-1} s^{-1} (μ_h / μ_e = 2.53) and 7.84× 10^{-4} /3.85 ×10^{-4} cm^2 V^{-1} s^{-1} (μ_h / μ_e = 2.03), respectively. For **PBDB-T: TPA-PDI$_3$** devices with better PCE, higher and more balanced mobilities are good for effective charge transport and thus acquire excellent J_{SC} and *FF*.

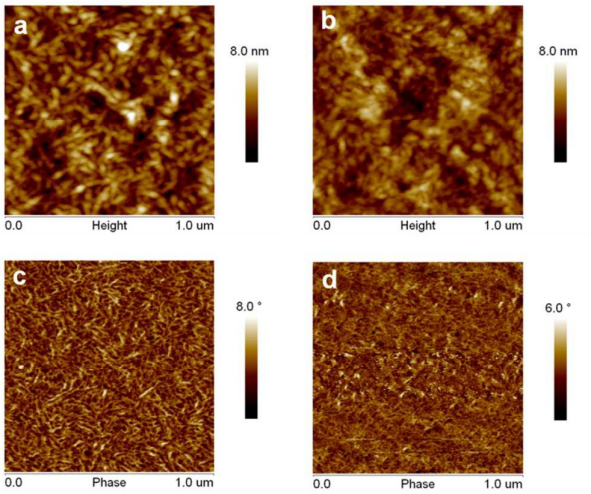

Figure 6. Atomic force microscopyheight and phase imagesof **PBDB-T:TPA-PDI$_2$** (a, c, 1:1, w/w) and **PBDB-T:TPA-PDI$_3$** (b, d, 1:1, w/w) blend film.

The unbalanced charge transport may be responsible for low EQE and *FF* observed for **TPA-PDI$_2$**.

2.6. Morphology characterization

The morphology of the BHJ films were known to closely correlate to mobility, J_{sc}, and finally PCE. Atomic force microscopy(AFM) with tapping mode was utilized to obtain the surface morphology of blend films. As illustrated from the height and phase images in Fig. 6, the root mean square (RMS) values of blend films of **PDBT-T: TPA-PDI$_2$** and **PDBT-T: TPA-PDI$_3$**are measured to be 1.07 and 0.92 nm, respectively. The lower RMS value for the **PBDB-T: TPA-PDI$_2$** and **PBDB-T: TPA-PDI$_3$** blend films indicate that the acceptor materials **TPA-PDI$_2$** and **TPA-PDI$_3$** have a good miscibility with **PBDB-T** molecule in the blend films, and may form a finer interpenetrating network, which facilitates both exciton separation and charge transport.[4g]

2.7. Photocurrent density and effective voltage study.

The exciton dissociation and charge extraction of **PBDB-T:TPA-PDI$_2$**and **PBDB-T:TPA-PDI$_3$** based OSCs were studied by measuring the photocurrent density (J_{ph}) versus effective voltage (V_{eff}). As shown in Fig. S4 and Table S5, the J_{ph}s of two OSCs reached saturation (J_{sat}) at voltages approaching 3 V, and the J_{sat} after annealing were 4.732 mA cm^{-2} and 10.875 mA cm^{-2} for **PBDB-T:TPA-PDI$_2$** and **PBDB-T:TPA-PDI$_3$**based OSCs, respectively. After annealing treatment, the probabilities of exciton dissociation calculated from J_{ph}/J_{sat} under the short circuit condition and probabilities of charge collection calculated from J_{ph}/J_{sat} at the maximal power output condition were 85.8% and 53.4% for **PBDB-T: TPA-PDI$_2$** based OSC, and 94.4% and 80.0% for **PBDB-T: TPA-PDI$_3$** based OSC, respectively. Obviously, the **PBDB-T: TPA-PDI$_3$** based OSC showed apparently higher exciton dissociation and charge

View Article Online
DOI: 10.1039/C8TC02823K

collection probabilities than those of **PBDB-T: TPA-PDI$_2$** based OSCs, which is beneficial for realizing a large J_{SC} and FF.

3. Conclusions

In conclusion, two novel small molecule acceptor **TPA-PDI$_2$** and **TPA-PDI$_3$** consisting of triphenylamine core and pyran-annulated perylene diimides (**Py-PDIs**) were designed and synthesized. Owing to the presence of the unique **TPA** core, **TPA-PDI$_2$** and **TPA-PDI$_3$** not only feature a rigid 3D conformation, but also presents suitable absorption properties and high electron mobility. The fabricated BHJ OSCs on the basis of **PBDB-T: TPA-PDI$_3$** show good performance with high PCE of up to 5.84%, which is the first report of of **Py-PDIs**-based non-fullerene acceptors. The result demonstrates that **Py-PDIs** is a promising building block for the construction of structurally non-planar **PDIs** derivatives as non-fullerene electron acceptors for highly efficient OSCs.

4. Experimental

4.1. General information

All solvents and chemicals used were purchased from Energy Chemical and used without further purification. TLC analyses were carried out by using Sorbent Technologies silica gel (200 mm) sheets. Column chromatography was performed on Sorbent silica gel 60 (40–63 mm). Solution NMR spectra were taken on a Bruker 400 MHz spectrometer in $CDCl_3$ at room temperature, both ^{1}H and ^{13}C NMR spectra were referenced to solvent residue peaks and the spectroscopic solvents were purchased from Cambridge Isotope Laboratories. Mass spectra were measured on a Bruker Maxis UHR-TOF MS spectrometer. UV–vis absorption spectra were performed with a Beijing Purkinje General Instrument Co. Ltd. TU-1901 spectrophotometer. Fluorescence spectra measurements were performed using FLS-920 Edinburgh fluorescence spectrometer. All steady-state measurements were carried out using a quartz cuvette with a path length of 1 cm. Element alanalyses (EA) were performed on a Flash EA 1112 elemental analyzer. Thermogravimetric analysis (TGA) was carried out on a TA Instrument TA Q50 the thermogravimetric Analyzer at a heating rate of 10 ^{o}C/min up to 600^{o}C.

4.2. Materials synthesis

PBDB-T was purchased from Organtec solar Materials Inc, M_n: 32 kDa; PDI = 2.5. **TPA-2EY** and **TPA-3EY** were synthesized according to the literature[13] with a modified method and shown in ESI.

4.2.1. Synthesis of Py-PDI-Br

To a mixture of **Py-PDI** (0.5 g, 0.5 mmol), $CHCl_3$ (50 mL) and K_2CO_3 (1.0 g，7.2 mmol) was added bromine (2.0 mL，0.4 mmol) at room temperature, then heated to reflux for 12 h and monitored by TLC. Then aq $NaHSO_3$ was added to quench excess bromine. After being extracted by CH_2Cl_2 and the combined organic phase was washed with brine. After removal of solvent, the residue was purified by silica gel column chromatography with petroleum ether/ CH_2Cl_2 (1:3)as the eluent to give compound **4** as a dark-red solid (0.4 g, 80% yield). ^{1}H NMR (300 MHz, $CDCl_3$, ppm): δ 9.85 (d, 1H), 8.73 (s, 1H), 8.57 (d, 1H), 8.49 (s, 1H), 8.03 (s, 1H), 4.10 (m, 2H), 1.84 (s, 6H), 1.32 (m, 64H), 0.86 (m, 12H). ^{13}C NMR (75 MHz, $CDCl_3$, ppm): δ 163.17, 162.29, 151.97, 139.46, 134.40, 128.16, 123.35, 120.35, 115.46, 80.27, 44.87, 44.73 36.70, 36.62, 31.94, 26.50, 22.70, 14.15. HRMS: $C_{67}H_{93}BrN_2O_5$ (M^++H), calcd, 1085.6268; found, 1085.6329.

4.2.2. Synthesis of TPA-PDI$_2$

Py-PDI-Br (407 mg, 0.375 mmol), **TPA-2EY** (50 mg, 0.17 mmol), $Pd(PPh_3)_4$ (100 mg) and CuI (20 mg) were added to a round bottom flask with the protection of Ar_2 gas, then dry toluene (20 mL) and dry diisopropylamine (5 mL) were injected into it. The reaction was stirred under 80 ^{o}C overnight. The cooled mixture was extracted with dichloromethane and water. The residue was purified by column chromatography (eluent, hexane/DCM, 60:1, 1:1) yielded compound **TPA-PDI$_2$** as a purple solid (123.7 mg, 31.4% yield).^{1}H NMR (400 MHz, $CDCl_3$, ppm): δ10.08 (d, 2H), 8.45 (s, 1H), 8.20 (d, 1H), 8.15(s, 1H) , 7.95 (s, 1H), 7.59 (d, 2H), 7.48 (t, 1H), 7.35-7.28 (m, 3H), 4.12-4.09 (m, 4H), 1.93(m, 2H), 1.78(m, 6H), 1.40-1.18(m, 64H) , 0.85-0.79 (m, 12H). ^{13}C NMR (400 MHz, $CDCl_3$, ppm): δ 163.35, 163.04, 162.92, 162.63, 151.61, 148.03, 145.90, 138.11, 134.07, 133.13, 132.69, 132.32, 130.24, 128.14, 126.80, 126.54, 125.75, 125.38, 125.02, 124.81, 124.60, 123.34, 123.07, 122.67, 122.30, 122.06, 120.75, 119.91, 116.14, 115.44, 102.15, 91.72, 80.07, 77.33, 77.02, 76.70, 44.84, 44.69, 36.80, 36.67, 31.92, 31.91, 31.84, 31.72, 30.13, 29.71, 29.68, 29.66, 29.38, 29.36, 27.98, 26.64, 26.54, 22.67, 22.66, 14.10. FT-IR (KBr, cm^{-1}): 2918, 2847, 2177, 1695, 1690, 1584, 1485, 1428, 1267. HRMS: $C_{156}H_{199}N_5O_{10}$ (M^+), calcd, 2303.5251, found 2303.5255. Analytical calculation for $C_{156}H_{199}N_5O_{10}$: C, 81.31; H, 8.70; N, 3.04;Experimental result: C, 80.78; H, 8.89;N 2.85 .

4.2.3. Synthesis of TPA-PDI$_3$

Py-PDI-Br (550 mg, 0.534 mmol), **TPA-3EY** (50 mg, 0.157 mmol), $Pd(PPh_3)_4$ (100 mg) and CuI (60 mg) were added to a round bottom flask with the protection of Ar_2 gas, then dry toluene (20 mL) and dry diisopropylamine (5 mL) were injected into it. The reaction was stirred under 80 ^{o}C overnight. The cooled mixture was extracted with dichloromethane and water. The residue was purified by column chromatography (eluent, hexane/DCM, 20:1, 1:1) yielded **TPA-PDI$_3$** as a purple solid (160 mg, 31% yield). ^{1}H NMR (400 MHz, $CDCl_3$, ppm): δ 10.22 (s, 1H), 8.46-8.24 (m, 3H), 7.77-7.75 (m, 3H), 7.38 (d, 2H), 4.10-4.07 (m, 4H), 1.93-1.80 (m, 8H), 1.26-1.11 (m, 64H), 0.83-0.73 (m, 12H). ^{13}C NMR (400 MHz, $CDCl_3$, ppm): δ 163.33, 163.11, 162.73, 162.36, 151.59, 146.98, 134.18, 133.38, 132.79, 132.29, 126.60,

View Article Online
DOI: 10.1039/C8TC02823K

125.30, 125.02, 124.54, 123.45, 122.98, 122.38, 120.55, 119.52, 115.35, 101.48, 92.21, 80.19, 31.92, 31.84, 31.69, 30.14, 30.10, 29.74, 29.72, 29.68, 29.66, 29.60, 29.58, 29.38, 29.30, 26.65, 26.48, 22.68, 22.60, 14.11, 14.09, 14.03. FT-IR (KBr, cm^{-1}): 2913, 2839, 2172, 1687, 1654, 1580, 1494, 1423, 1267, 1164. HRMS: $C_{225}H_{291}N_7O_{15}$ (M^+), calcd, 3333.2290, found 3333.2343. Analytical calculation for$C_{225}H_{291}N_7O_{15}$: C, 81.06; H, 8.80; N, 2.94; Experimental result: C, 80.88; H , 8.79; N 2.95.

4.3. Computational method

The geometry was optimized by density functional theory (DFT) using the B3LYP hybrid functional with basis set 6-31G(d).[16]Quantum chemical calculation was performed with the Gaussian09 package. The long alkyl chains were replaced with an isopropyl group for simplification.

4.4. Device fabrication and characterization

Solar cells were fabricated in a conventional device configuration of ITO/PEDOT: PSS/active layer/Zracac/Al. The ITO substrates were first scrubbed by detergent and then sonicated with deionized water, acetone and isopropanol subsequently, and dried overnight in an oven. The glass substrates were treated by UV-Ozone for 20 min before use. PEDOT: PSS (Heraeus Clevios P VP A 4083) layer was spin-cast onto the ITO substrates at 4000 rmp for 40s, and then dried at 150 °C for 10 min in air. The donor:acceptor blends with 1:1 ratio were dissolved in *O*-dichlorobenzene (the concentration of blend solutions are 20 mg/mL for all blend films), and stirred overnight in a nitrogen-filled glove box. The blend solution was spin-cast at 1600 rmp for 40 s on the top of PEDOT: PSS layer followed by annealed at 100 °C for 5 min to remove the residual solvent. A thin Zracac layer (10 nm) and Al layer (100 nm) were sequentially evaporated through a shadow mask under vacuum of 5×10^{-5} Pa. The active area is 4.50 mm^2. The area of each device was 3.14 mm^2 defined by a shadow mask. The optimal blend thickness was about 95 nm, measured on a Bruker Dektak XT stylus profilometer. Current density-voltage (J-V) curves were measured in a Keithley 2400 Source Measure Unit. Photocurrent was measured in an Air Mass 1.5 Global (AM 1.5 G) solar simulator (Class AAA solar simulator, Model 94063A, Oriel) with an irradiation intensity of 100 mW cm^{-2}, which was measured by a calibrated silicon solar cell and a readout meter (Model 91150V, Newport). EQE spectra were measured by using a QEX10 Solar Cell EQE measurement system (PV measurements, Inc.).

Conflicts of interest

There are no conflicts to declare.

Acknowledgements

B. Tang acknowledges the National Natural Science Foundation of China (No. 21390411, 21535004, 91753111). G. Li acknowledges the financial support from start-up grant of Shandong Normal University and Shandong Province Natural Science Foundation (ZR2016BM24).

Notes and references

1 (a) G. Yu, J. C. Hummelen, F. Wudl and A. J. Heeger, *Science*, 1995, **270**, 1789; (b) G. Zhang, J. Zhao, P. C. Y. Chow, K. Jiang, J. Zhang, Z. Zhu, J. Zhang, F. Huang and H. Yan, *Chem. Rev.*, 2018, **118**, 3447; (c) G. Li, R. Zhu and Y. Yang, *Nat. Photonics*, 2012, **6**, 153; (d) A. J. Heeger, *Adv. Mater.*, 2014, **26**, 10.

2 (a) J. Zhao, Y. Li, G. Yang, K. Jiang, H. Lin, H. Ade, W. Ma and H. Yan, *Nat. Energy*, 2016, **1**, 15027; (b) M. Li, K. Gao, X. Wan, Q. Zhang, B. Kan, R. Xia, F. Liu, X. Yang, H. Feng, W. Ni, Y. Wang, J. Peng, H. Zhang, Z. Liang, H.-L. Yip, X. Peng, Y. Cao and Y. Chen, *Nat. Photonics*, 2016, **11**, 85.

3 J. Hou, O. Inganäs, R. H. Friend and F. Gao, *Nat. Materials*, 2018, **17**, 119.

4 (a) H. Choi, S. J. Ko, T. Kim, P. O. Morin, B. Walker, B. H. Lee, M. Leclerc, J. Y. Kim and A. J. Heeger, *Adv. Mater.*,2015, **27**, 3318; (b) S. Holliday, R. S. Ashraf, C. B. Nielsen, M. Kirkus, J. A. Röhr, C.-H. Tan, E. Collado-Fregoso, A.-C. Knall, J. R. Durrant, J. Nelson and I. McCulloch, *J. Am. Chem.Soc.,* 2015, **137**, 898; (c) Y. Lin, Z.-G. Zhang, H. Bai, J. Wang, Y. Yao, Y. Li, D. Zhu and X. Zhan, *Energy Environ. Sci.,* 2015, **8**, 610; (d)S. Holliday, R. S. Ashraf, A. Wadsworth, D. Baran, S. A. Yousaf, C. B. Nielsen, C.-H. Tan, S. D. Dimitrov, Z. Shang, N. Gasparini, M. Alamoudi, F. Laquai, C. J. Brabec, A. Salleo, J. R. Durrant and I. McCulloch, *Nat. Commun.,* 2016, **7**, 11585; (e) Y. Lin, F. Zhao, Q. He, L. Huo, Y. Wu, T. C. Parker, W. Ma, Y. Sun, C. Wang, D. Zhu, A. J. Heeger, S. R. Marder and X. Zhan, *J. Am. Chem.Soc.,* 2016, **138**, 4955;(f)J. Liu, S. Chen, D. Qian, B. Gautam, G. Yang, J. Zhao, J. Bergqvist, F. Zhang, W. Ma, H. Ade, O. Inganäs, K. Gundogdu, F. Gao and H. Yan, *Nat. Energy,* 2016, **1**, 16089. (g) Y. Liu, Y. Yang, C.-C. Chen, Q. Chen, L. Dou,Z. Hong, G. Liand Y. Yang, *Adv. Mater.*, 2013, **25**, 4657.(h) Y. Lin, J. Wang, Z. - G. Zhang, H. Bai, Y. Li, D. Zhu and X, Zhan,*Adv. Mater.,* 2015, **27**, 1170. (i) C. Yan, S. Barlow, Z. Wang, H. Yan, A. K.-Y. Jen, S. R. Marder and X. Zhan, *Nat. Rev. Mater.*, 2018, **3**, 18003.(j) J. Zhu, Z. Ke, Q. Zhang, J. Wang, S. Dai, Y. Wu, Y. Xu, Y. Lin, W. Ma, W. You and X.i Zhan, *Adv. Mater.*, 2018, **30**, 1704713. (k) Y. Lin, Y. Wang, J. Wang, J. Hou, Y. Li, D. Zhu and X. Zhan, *Adv. Mater.,* 2014, **26**, 5137. (l) X. Zhan, A. Facchetti, S. Barlow, T. J. Marks, M. A. Ratner, M. R. Wasielewski and S. R. Marder, *Adv. Mater.,* 2011, **23**, 268. (m) Y. Lin, F. Zhao, S. K. K. Prasad, J.-D. Chen, W. Cai, Q. Zhang, K. Chen, Y. Wu, W. Ma, F. Gao, J.-X. Tang, C. Wang, W. You, J. M. Hodgkiss and X. Zhan, *Adv. Mater.*, 2018, **30**, 1706363. (n) Q. Wu, D. Zhao, J. Yang, V. Sharapov, Z. Cai, L. Li, N. Zhang, A. Neshchadin, W. Chen and L. Yu, *Chem. Mater*, 2017, **29**, 1127.

5 (a) B. Fan, K. Zhang, X. F. Jiang, L. Ying, F. Huang and Y. Cao, *Adv. Mater.*, 2017, **29**, 1606396; (b) Z. Li, X. Xu, W. Zhang, X. Meng, Z. Genene, W. Ma, W. Mammo, A. Yartsev, M. R. Andersson, R. A. J. Janssen and E. Wang, *Energy Environ. Sci.,* 2017, **10**, 2212; (c) Y. Liu, Z. Zhang, S. Feng, M. Li, L. Wu, R. Hou, X. Xu, X. Chen and Z. Bo, *J. Am. Chem.Soc.,* 2017, **139**, 3356; (d)A. Mishra, M. Keshtov, A. Looser, R. Singhal, M. Stolte, F. Wurthner, P. Bauerle and G. D. Sharma, *J.Mater. Chem. A.,*2017, **5**, 14887; (e) Z. Xiao, X. Jia and L. Ding, *Sci. Bul.,* 2017, **62**, 1562; (f) H. Yao, Y. Cui, R. Yu, B. Gao, H. Zhang and J. Hou, *Angew. Chem., Int. Ed.,* 2017, **56**, 3045; (g) J. Zhang, Y. Li, J. Huang, H. Hu, G. Zhang, T. Ma, P. C. Y. Chow, H. Ade, D. Pan and H. Yan, *J. Am. Chem.Soc.,*2017, **139**, 16092; (h) W. Zhao, S. Li, H. Yao, S. Zhang, Y. Zhang, B. Yang and J. Hou, *J. Am. Chem.Soc.,* 2017, **139**, 7148; (i) Z. Luo, H.

View Article Online
DOI: 10.1039/C8TC02823K

Bin, T. Liu, Z. G. Zhang, Y. Yang, C. Zhong, B. Qiu, G. Li, W. Gao, D. Xie, K. Wu, Y. Sun, F. Liu, Y. Li and C. Yang, *Adv. Mater.*, 2018, **30**, 1706124; (j)T. Liu, D. Meng, Y. Cai, X. Sun, Y. Li, L. Huo, F. Liu,Z. Wang, T. P. Russell, Y. Sun, *Adv. Sci*, 2016, **3**, 1600117; (k) Q. Tao, T. Liu, L. Duan, Y. Cai, W. Xiong, P. Wang, H. Tan, G. Lei, Y. Pei, W. Zhu, R. Yang and Y. Sun, *J.Mater. Chem. A.,* 2016, **4**, 18792; (l)T. Liu, L. Huo, S. Chandrabose, K. Chen, G. Han, F. Qi,X. Meng, D. Xie, W. Ma, Y. Yi, J. M. Hodgkiss, F. Liu,J. Wang, C. Yang and Y. Sun, *Adv. Mater.*, 2018, **30**, 1707353.

6 (a) Z. Zheng, O. M. Awartani, B. Gautam, D. Liu, Y. Qin, W. Li, A. Bataller, K. Gundogdu, H. Ade and J. Hou, *Adv. Mater.*,2017, **29**, 1604241; (b) H. Bin, L. Gao, Z.-G. Zhang, Y. Yang, Y. Zhang, C. Zhang, S. Chen, L. Xue, C. Yang, M. Xiao and Y. Li, *Nat. Commun.,*2016, **7**, 13651; (c) C. Sun, F. Pan, H. Bin, J. Zhang, L. Xue, B. Qiu, Z. Wei, Z.-G. Zhang and Y. Li, *Nat. Commun.,* 2018, **9**, 743.

7 Y. Duan, X. Xu, H. Yan, W. Wu, Z. Li and Q. Peng, *Adv. Mater.*, 2017, **29**, 1605115.

8 (a) Q. Wu, D. Zhao, A. M. Schneider, W. Chen and L. Yu, *J. Am. Chem.Soc.,*2016, **138**, 7248; (b) H. Wang, L. Chen and Y. Xiao, *J.Mater. Chem. A.,* 2017, **5**, 22288; (b) Y. Liu, C. Mu, K. Jiang, J. Zhao, Y. Li, L. Zhang, Z. Li, J. Y. L. Lai, H. Hu, T. Ma, R. Hu, D. Yu, X. Huang, B. Z. Tang and H. Yan, *Adv. Mater.*, 2015, 27, 1015; (c) Y. Zhong, M. T. Trinh, R. Chen, G. E. Purdum, P. P. Khlyabich, M. Sezen, S. Oh, H. Zhu, B. Fowler, B. Zhang, W. Wang, C.-Y. Nam, M. Y. Sfeir, C. T. Black, M. L. Steigerwald, Y.-L. Loo, F. Ng, X. Y. Zhu and C. Nuckolls, *Nat. Commun.,* 2015, **6**, 8242.

9 (a) J. Lee, R. Singh, D. H. Sin, H. G. Kim, K. C. Song and K. Cho, *Adv. Mater.*, 2016, **28**, 69; (b) S.-Y. Liu, C.-H. Wu, C.-Z. Li, S.-Q. Liu, K.-H. Wei, H.-Z. Chen,A. K.-Y. Jen, *Adv. Sci.,* 2015, **2**, 1500014.

10 A. Zhang, C. Li, F. Yang, J. Zhang, Z. Wang, Z. Wei and W. Li, *Angew. Chem., Int. Ed.,* 2017, **56**, 2694.

11 (a) D. Sun, D. Meng, Y. Cai, B. Fan, Y. Li, W. Jiang, L. Huo, Y. Sun and Z. Wang, *J. Am. Chem.Soc.,*2015, **137**, 11156; (b) D. Meng, D. Sun, C. Zhong, T. Liu, B. Fan, L. Huo, Y. Li, W. Jiang, H. Choi, T. Kim, J. Y. Kim, Y. Sun, Z. Wang and A. J. Heeger, *J. Am. Chem.Soc.,* 2016, **138**, 375; (c) A. D. Hendsbee, J.-P. Sun, W. K. Law, H. Yan, I. G. Hill, D. M. Spasyuk and G. C. Welch, *Chem. Mater.,* 2016, **28**, 7098. (d) Z. Luo, T. Liu, W. Cheng, K. Wu, D. Xie, L. Huo, Y. Sun and C. Yang, *J.Mater. Chem. C.,* 2018, **6**, 1136. (e) T. A. Welsh, A. Laventure, T. Baumgartner and G. C. Welch, *J.Mater. Chem. C.,* 2018, **6**, 2148. (f) J. Cann, S. Dayneko, J.-P. Sun, A. D. Hendsbee, I. G. Hill and G. C. Welch, *J.Mater. Chem. C.,* 2017, **5**, 2074.

12 (a) R. Wang, G. Li, A. Zhang, W. Wang**,** G. Cui, J. Zhao, Z. Shi and B. Tang,*Chem. Commun.*, 2017, **53**, 6918; (b) R. Wang, Y. Ma, J. Zhao, A. Zhang, S. Yang, H. Shen, G. Li and Z. Shi, *Sens. Actuators. B. Chem.,* 2018, **260**, 719.

13 (a) A. Chowdhury, P. Howlader and P. S. Mukherjee, Chem.-Eur. J. 2016, 22, 7468; (b) P. Z. Li, X. J. Wang, S. Y. Tan, C. Y. Ang, H. Chen, J. Liu, R. Zou and Y. Zhao, *Angew. Chem., Int. Ed.,* 2015, **54**, 12748.

14 Z. Luo, T. Liu, W. Cheng, K. Wu, D. Xie, L. Huo, Y. Sun and C. Yang, *J.Mater. Chem. C.,* 2018, **6**, 1136.

15 Z. Yao, X. Liao, K. Gao, F. Lin, X. Xu, X. Shi, L. Zuo, F. Liu, Y. Chen and A. K. Y. Jen, *J. Am. Chem.Soc.* 2018, **140**, 2054.

16 M. J. Frisch, G. W. Trucks, H. B. Schlegel, G. E. Scuseria, M. A. Robb, J. R. Cheeseman, G. Scalmani, V. Barone, G. A. Petersson, H. Nakatsuji, X. Li, M. Caricato, A. Marenich, J. Bloino, B. G. Janesko, R. Gomperts, B. Mennucci, H. P. Hratchian, J. V. Ortiz, A. F. Izmaylov, J. L. Sonnenberg, D. Williams-Young, F. Ding, F. Lipparini, F. Egidi, J. Goings, B. Peng, A. Petrone, T. Henderson, D. Ranasinghe, V. G. Zakrzewski, J. Gao, N. Rega, G. Zheng, W. Liang, M. Hada, M. Ehara, K. Toyota, R. Fukuda, J. Hasegawa, M. Ishida, T. Nakajima, Y. Honda, O. Kitao, H. Nakai, T. Vreven, K. Throssell, J. A. Montgomery, Jr., J. E. Peralta, F. Ogliaro, M. Bearpark, J. J. Heyd, E. Brothers, K. N. Kudin, V. N. Staroverov, T. Keith, R. Kobayashi, J. Normand, K. Raghavachari, A. Rendell, J. C. Burant, S. S. Iyengar, J. Tomasi, M. Cossi, J. M. Millam, M. Klene, C. Adamo, R. Cammi, J. W. Ochterski, R. L. Martin, K. Morokuma, O. Farkas, J. B. Foresman, and D. J. Fox, Gaussian 09, revision A.1; Gaussian, Inc.: Wallingford, CT, 2009.

View Article Online
DOI: 10.1039/C8TC02823K

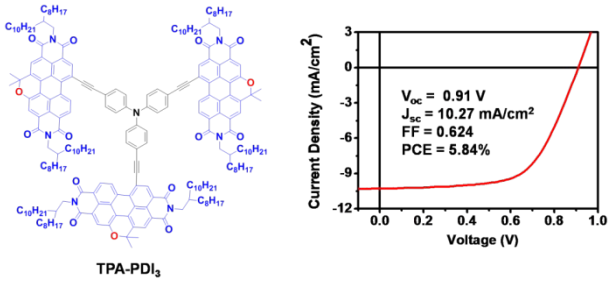

Through the coupling of acetylene substituted triphenylamine and pyran-annulated perylene diimides, two novel non-fullerene electron acceptors, coded as **TPA-PDI$_2$** and **TPA-PDI$_3$**, were designed, synthesized and applied in BHJ organic solar cells.